

# The UV spectrum of nebulae

Frédéric Zagury <sup>1</sup>

*Department of Astrophysics, Nagoya University, Nagoya, 464-01 Japan* <sup>2</sup>

Received 24 February 2000; accepted 14 April 2000

---

## Abstract

This paper presents an analysis of the UV spectrum of some nebulae with clearly identified illuminating stars, all observed by the IUE satellite.

The data show remarkable properties of the UV spectrum of the nebulae. Each spectrum is the product of the star spectrum and a linear function of  $1/\lambda$ . There is no peculiar behaviour in the spectrums at 2200 Å: no bump created in the spectrum of a nebula and no excess of scattering. When moving away from the star, the surface brightness of a nebula decreases as the inverse of the square of the angular distance to the star.

These results can logically be interpreted in terms of scattering of starlight. They imply constant properties of the interstellar grains in the UV and in the directions of space sampled by the nebulae, and probably a strong forward scattering phase function. There is no evidence for any particular type of grain which would specifically extinguish starlight at 2200 Å.

Concerning the UV spectrum of a star, this may imply a revisal of the traditional interpretation of the 2200 Å bump.

---

## 1 Introduction

In the UV, as in the optical, the light which we receive from a nebula should in great part be the light of the illuminating star scattered by dust grains in the nebula. If no other process than scattering of starlight by the average population of interstellar grains is involved, the ratio of the nebula to the star spectrum depends on the optical depth of the nebula, on the angle  $\varphi$  of scattering, and on the albedo and phase function of interstellar grains.

---

<sup>1</sup> Supported by the Japanese Society for the Promotion of Science, grant ID No P97234.

<sup>2</sup> E-mail: zagury@a.phys.nagoya-u.ac.jp

The original idea of this work was to study the behavior of the spectrum of nebulae in the 2200 Å region. In this spectral region, the spectrum of the stars is known to have a characteristic depression (the 2200 Å bump) when there is interstellar matter between the star and the observer. The possible causes of the bump are reviewed by Bless & Savage [1]. Admittedly, the bump is an extinction feature (eventually a purely absorbing one, Witt et al. [9]) which arises due to a particular type of interstellar grain.

Since a nebula placed in front of a star produces a bump in the spectrum of the star, what will the bump spectral region of a nebula illuminated by a star at close angular distance be? If the particles which extinguish starlight at 2200 Å are present in the nebula, its spectrum should have an evident feature at 2200 Å. This feature will be an absorption one if the bump carriers are purely absorbing particles. It will be an excess of emission if the carriers scatter starlight.

Section 2 presents the IUE observations used in this work. It consists of the spectrums of a few well known nebulae, all illuminated by close bright stars.

Section 3 to Section 4, is an analysis of the data. It is a remarkable fact, and the most significant result of this analysis, that all the nebulae have a spectrum which is exactly the product of the illuminating star spectrum and a linear function of  $1/\lambda$  (Section 3). Some nebulae do not have a bump, and when they do have one it is always proportional to the bump of the illuminating star. No bump is created in the nebulae.

In Section 5, the relation between the spectrum of a nebula and the spectrum of the illuminating star is interpreted as scattering of starlight by a medium with an optical depth which varies as  $1/\lambda$ .

A second result, the power law dependence of the surface brightness on the angular distance to the star, is arrived at and discussed in Sections 4 and 6. The large variations of the surface brightness level of a nebula with the distance to the star may be an important argument in favor of a strong forward scattering phase function in the UV (Section 6). It implies that a considerable amount of starlight is scattered in directions close to the star.

Different authors (e.g. A.N. Witt and collaborators) have found a strong forward scattering phase function of the grains in the UV. These papers are associated with models which also predict changes of the albedo and/or the phase function with the wavelength. From analysis of the present data, I cannot agree with these conclusions. Contrary to these studies, I find constant albedo and phase function of the grains in all the UV, and perhaps up to the near infrared, in all directions of space. In Section 7, a few of these papers are briefly discussed along with the consequences the present paper have on the properties of interstellar grains. It is suggested that there is no excess of

extinction in the spectrum of the stars at 2200 Å.

An Appendix will review elementary properties of scattering and the notations used in the paper.

## 2 Data

### 2.1 IUE data

All the observations used in this paper were made by the International Ultraviolet Explorer. The IUE satellite and the detector system are described by Boggess et al. [2,3]. Recent and complete information on the project and data reduction are available at the IUE website: <http://iuearc.vilspa.esa.es>. The camera has two entrance apertures and two dispersion modes. Observations can be made through a large aperture ( $L$ ),  $10'' \times 20''$  wide, or through a small one, ( $S$ ),  $3''$  large in diameter.  $S$ -aperture observations of a star generally need to be multiplied by a factor of 1.2 to 2 to match  $L$ -aperture observations of the same star. The difference is attributed to the difficulty of holding the star within the beam when using the small aperture. Observations can be made in a low resolution mode of  $\sim 7$  Å or with a higher spectral resolution of 0.1–0.2 Å. Three cameras: the LWR, the LWP, and the SWP, have been used during the 20 year-long existence of the satellite. The SWP camera covers the wavelength range [1150 Å, 1980 Å], while the LWR and the LWP cameras cover the [1850 Å, 3350 Å] range. The LWR camera was the ‘standard’ long wavelength camera from the beginning of the mission up until October 1983. A problem with the camera’s electronic led to a switch to the LWP. The total range in wavelengths is from 1150 Å to 3350 Å. The data at both boundaries should be carefully considered.

An IUE spectrum gives the power per unit surface and per wavelength received by the satellite in the U.V. from the direction of a celestial object. A typical extracted spectrum has the  $y$ -coordinate in absolute flux units ( $\text{erg}/\text{cm}^2/\text{s}/\text{Å}$ ) and the  $x$ -coordinate in Å. The sensitivity of the observations is limited to a few  $10^{-15}$   $\text{erg}/\text{s}/\text{cm}^2/\text{Å}$ .

The IUE data cannot be used straight away. A transfer function, which is to be applied to the raw data, and which considerably modifies the original data files, is provided by the IUE data reduction team.

I have used the .MLXO and .MXHI files which were up until recently available at the IUE website. Those files are the final products of the processing from raw data to final spectrums. Following IUE recommendations, the files were

Name	$\alpha_{1950}$ h m s	$\delta_{1950}$ ° ′ ″	star	$E$	$d_\theta$ ″	$(F_N/F_\star)_m$ $\times 10^{-3}$	$R^1$	$R\theta^2$ $\times 10^{-3}$
17 $\tau$ nebula	03 41 55	+23 57 10	HD 23302	0.047	18	1.81	0.56	2.93
Orion nebula 1	05 38 18	−02 01 05	HD 37742	0.07	193	0.0154	0.57	2.86
Orion nebula 2	05 38 22	−02 03 05	HD 37742	0.07	326	0.0048	0.51	2.56
Orion nebula 3	05 38 34	−02 09 05	HD 37742	0.07	727	$8.5 \times 10^{-4}$	0.45	2.25
Merope nebula 1	03 43 21	+23 46 39	HD 23480	0.089	60	0.37	1.32	6.64
Merope nebula 2	03 43 21	+23 47 19	HD 23480	0.089	20	3.82	1.53	7.64
20 $\tau$ nebula 1	03 42 50	+24 12 26	HD 23408	0.041	22	1.98	0.96	4.79
NGC 2023	05 39 06	−02 17 24	HD 37903	0.32	26	14.98	10.12	50.63
IC 435	05 40 30	−02 19 48	HD 38087	0.25	17	7.98	2.31	11.53
20 $\tau$ nebula 2	03 42 51	+24 12 32	HD 23408	0.041	15	3.99	0.90	4.49
NGC 7023	21 00 56	+67 57 49	HD 200775	0.55	20	1.07	0.44	2.2
CED 201	22 12 17	+70 00 25	BD +69 1231	0.16	15	10.98	4.39	12.35

Table 1

Main parameters for the nebulae presented in the paper. Nebulae are listed by increasing optical depth. The table gives the adopted name of the nebula; coordinates of IUE nebula observations; its illuminating star;  $E = E(B - V)$  in the star direction; angular distance to the star; maximum observed ratio of nebula to star fluxes,  $(F_N/F_\star)_m$ ;  $(F_N/F_\star)_m$  rescaled to a distance of 1″:  $R^1 = (F_N/F_\star)_m^{1''}$ ; and  $R = (F_N/F_\star)_m^{1''} / 200''^2$ .

read by the IDL software readmx.pro procedure provided in the IUE package NEWSIPS for IDL.

## 2.2 Data used in this paper

I have used the spectrums of nebulae (IUE class 73) and of stars. For each object, the spectrum presented in the paper is an average of the best observations of the object. I sometimes used high dispersion spectrums and decreased the resolution by using a median filter.

Observations of nebulae with clearly identified illuminating sources are not so frequent. Most were studied although they are not all presented here. The results of the paper hold for the other nebulae as well.

The main properties of the nebulae are summarized in Table 1. I found it unnecessary to specify the IUE observations' name of the objects listed, since

they can easily be looked at or retrieved from the IUE website. A reference list of the IUE images is available upon request.

All nebulae were observed at different distances to the star. Different observations of a nebula with the same camera are often proportional when the position of the observations are close. This proportion is justified by the proximity of the observations and indicates equal optical depths and similar mediums. They may differ when the positions are too far apart due to modifications of the nature of the interstellar medium. When different positions to the star were exactly proportional, I chose to present either the best spectrum or the average one, so as to reduce the noise. Regions illuminated by the same star, with spectrums which cannot be superimposed, were considered as separate nebulae.

The spectrums of the same object taken with the SWP camera or with one of the long wavelength range cameras usually join in the common spectral region ( $\sim 1900\text{--}2000\text{ \AA}$ ). A slight gap between the long and the short wavelength spectrums sometimes happens and has been attributed either to a calibration problem or to a problem of precision in the pointing. In this case a correcting factor was applied to the long wavelengths' range spectrum to ensure continuity from one range of wavelengths to another. This scaling has no effect on the relations which will be obtained between the spectrums of a nebula and that of its illuminating star since these relations apply individually to each camera.

### 3 Comparison of the spectrums of the nebulae with that of the stars

#### 3.1 Nebulae with no bump

Fig. 1, left, plots the spectrum of a nebula and its illuminating star, HD 23302 ( $17\tau$ ), as a function of  $\lambda$ . The two bottom plots are two positions observed by the IUE satellite in the Orion nebula. In both cases, the illumination is due to HD 37742, a few arcminutes apart. An intermediate position, Orion nebula 2, not represented here, was also observed. The spectrum of the Orion nebula 2 matches the Orion nebula 1 spectrum when multiplied by 3.

Stars and nebulae spectrums are not proportional, but Fig. 1 shows that the spectrum of a nebula is exactly overlaid by the spectrum of the illuminating star, after multiplication by a linear function of  $1/\lambda$ .

It is worth noticing that no bump is created in the nebulae.

### 3.2 General relation between the UV spectrums of a nebula and that of the illuminating star

The preceding fit of the emission of a nebula by the product of the illuminating star flux and a linear function of  $1/\lambda$  can successfully be repeated for all the nebulae observed by the IUE satellite, whether they have a bump or not. Fig. 2 shows the results for 8 nebulae and gives 3 coefficients,  $(k, a, b/a)$ .  $k$  is the coefficient of the zero order fit, restricted to the long wavelength's range, of the spectrum of the star to the nebula spectrum. The star spectrum, after smoothing by a median filter for sake of clarity, is multiplied by  $k$  and represented by the curve in dashes. The nebula spectrum is in dots. It is fitted by the star spectrum multiplied by a linear function of  $1/\lambda$ , the overlaid solid line curve. The relation between the spectrums can always be written as:

$$F_N \sim \alpha F_\star \left( a \frac{1 \mu\text{m}}{\lambda} - b \right), \quad (1)$$

where  $F_N$  and  $F_\star$  are the nebula and the star fluxes measured by the IUE satellite.  $\alpha$  is a coefficient which must depend on the albedo and the phase function of interstellar grains and on the relative position of the star, the nebula and the observer.  $a$  can be 0, 1 or  $-1$ .

The relation which is found between the UV emission of a nebula and its illuminating star should still apply to their UV fluxes corrected for foreground extinction: the star and the nebula are close enough to be equally (in proportion of their flux) affected by interstellar material situated between the star and the nebula on the one hand and the observer on the other hand. Since they are proportional, the bumps of a nebula and its illuminating star should be attributed to dust in front of both the nebula and the star.

## 4 Strength and variation of UV surface brightness of the nebulae with distance to the star

The proportion of starlight which is scattered by a nebula is evaluated by the  $R = S/F_\star$  parameter.  $R$  can theoretically be defined as the ratio of the nebula surface brightness to the star flux, both measured at the same position and corrected for foreground extinction. Slight or no reddening of the star's light between the star and the scattering volume should also be assumed.

The maximum proportion of starlight which can be scattered in the direction  $\varphi$  is given by  $R_{max} = S_{max}/F_\star$ , where  $S_{max}$  is the maximum surface brightness the nebula can reach (corresponding to an optical depth  $\tau_{max} \sim 1 - 2$ ) at  $\varphi$ .

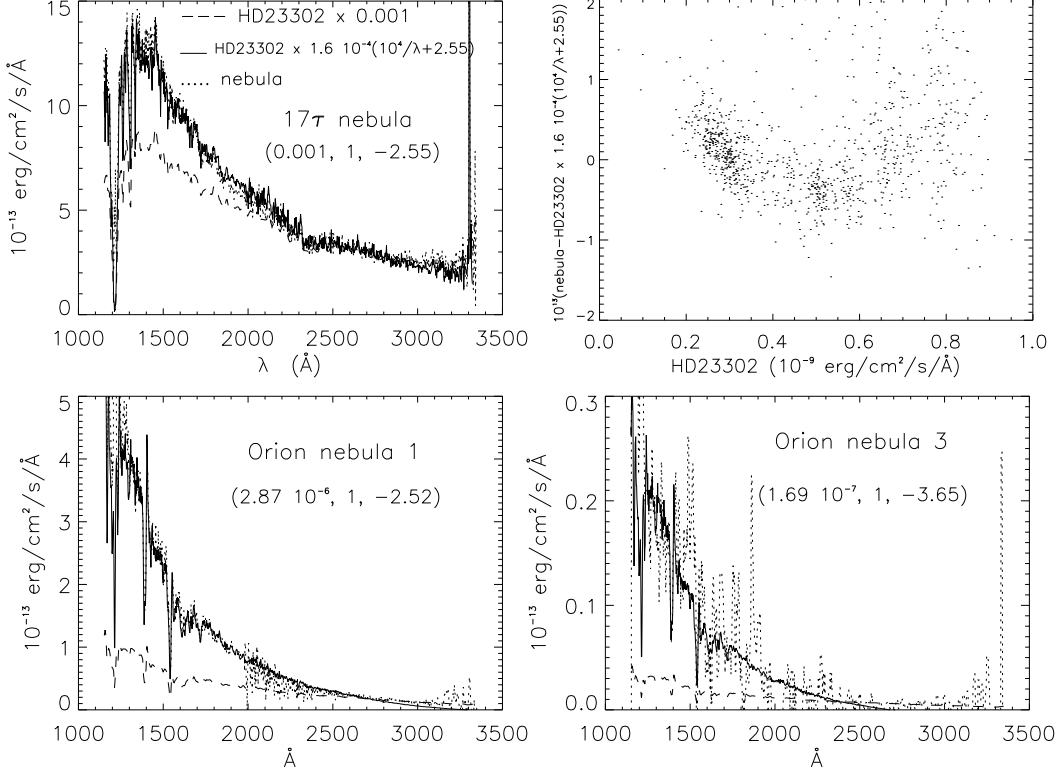


Fig. 1. *Top left*: The spectrum of the 17 $\tau$  nebula, in dots, is overlaid by the product of the star spectrum and a linear function in  $1/\lambda$ . Underneath, the star spectrum (in dashes) was scaled to the nebula’s in the long wavelength range. *Top right*: Difference between the star-fit to the nebula and the nebula spectrums, plotted versus the star spectrum. There is no residual correlation. *Down*: Spectrums of Orion nebulae 1 and 3 and of the illuminating star HD 37742. Dash, dot and solid lines have the same meaning as for the 17 $\tau$  nebula. The signification of the numbers in parenthesis is given in Section 3.2.

$R_{max}$  depends solely on the angle of scattering  $\varphi$ .

Column 5 of Table 1 gives the non-dimensional quantity  $R\theta^2$  for each of the observations.  $R\theta^2$  was estimated by taking the maximum value (over the [1000 $\text{\AA}$ , 3000 $\text{\AA}$ ] IUE wavelength range) of  $(F_N/F_\star)(\theta^2/A_{IUE})$ , the ratio of the maximum surface brightness of the nebula to the star flux, normalized to a distance of  $\theta = 1''$  to the star.  $A_{IUE} = 200 \text{ arcsec}^2$  is the surface of the IUE camera large aperture. If, as will be suggested in Sect. 5.1, the mean optical depth of the nebulae is close to  $\tau_{max}$ ,  $R\theta^2$  should be close to  $R_{max}\theta^2$ .

The range of values the observed maximum of  $R\theta^2$  takes (last column of Table 1) is quite narrow. Within the restrictions due to the margin of error discussed in the following section,  $R_{max}\theta^2$  can be taken to be  $\sim 3 \times 10^{-3}$ , for  $\theta$  between  $\sim 10''$  and a few arcminutes. From the present data, it is not possible to discern whether the observed maximum of  $R\theta^2$  in Table 1 is a constant or varies with the nebula.

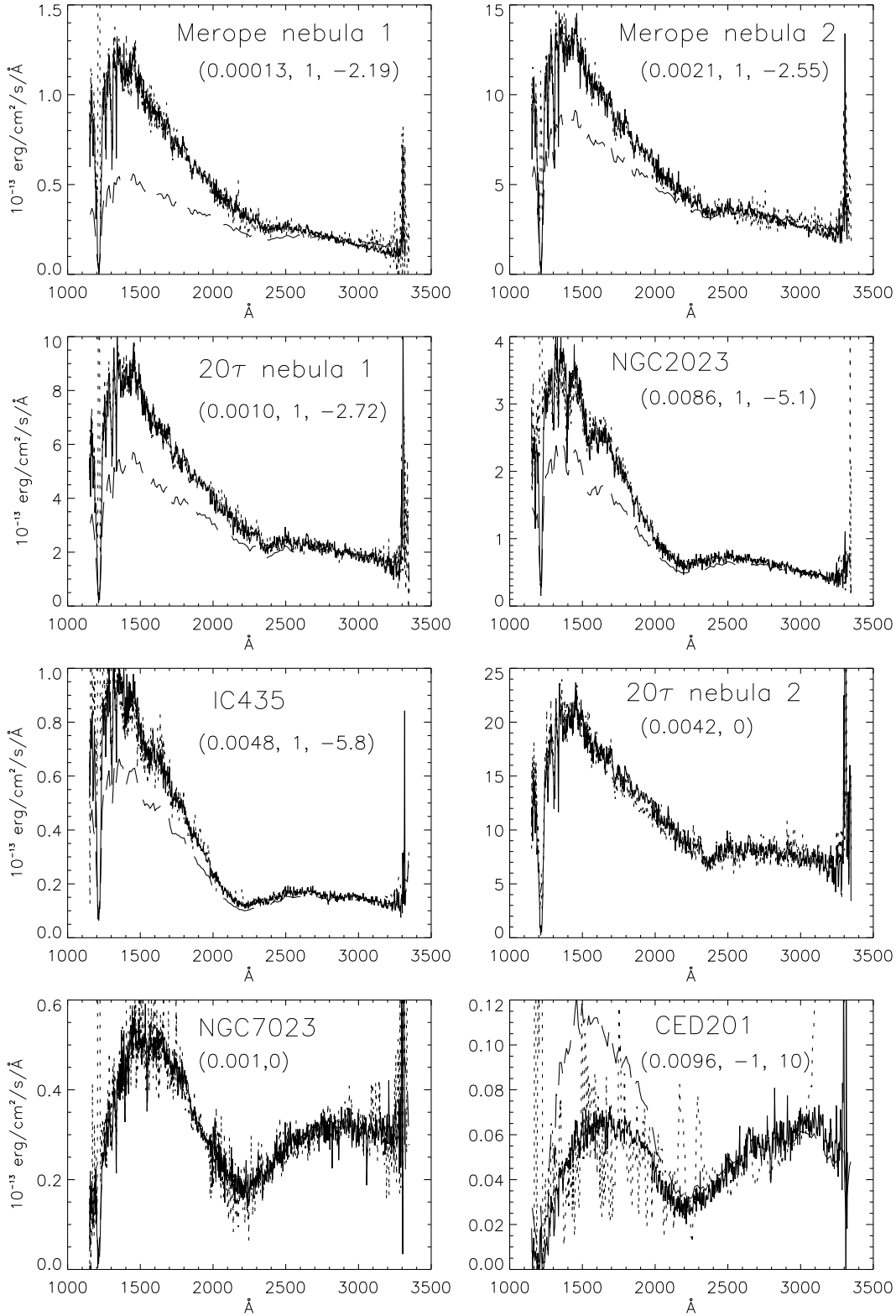


Fig. 2. Spectrums of 8 nebulae and of their illuminating star. For each plot the nebula spectrum is in dots, the star spectrum (smoothed and scaled by  $k$  to fit the nebula spectrum at long wavelengths) in dashes, and the star spectrum fitted to the nebula's in solid line. The coefficients are  $(k, a, b/a)$ ,  $k$  defined above and  $(a, b)$  from Eq. (1). When  $a = 0$ ,  $b = \infty$  is omitted. The nebulae are presented by order of increasing average optical depth from left to right and top to bottom.



Table 1 suggests a power law dependence of the nebulae surface brightness with angular distance to the illuminating star. For the observations of nebulae in the same region (e.g. Orion, Merope and  $20\tau$  nebulae), illuminated by the same star,  $R\theta^2$  is remarkably constant.

When different positions of the same nebula are available and proportional, the data show that there are strong variations of the brightness with angular distance to the star but  $R\theta^2$  stays relatively constant.

#### 4.1 Sources of error on the evaluation of the $R$ coefficient

Differences between the observed values of  $R$ , reported in the Table 1, and its theoretical definition can arise from a mistaken evaluation of either the nebula surface brightness or the unreddened flux of the star.

A major difficulty when estimating the exact surface brightness is the width of the beam of the observations, which in many cases has dimensions comparable to the distance to the star. It should be reliable when the dimensions of the beam are small compared to the distance to the star but errors may arise when the observation is made at close distance to the star (a few  $10''$ ). In the latter case, the variation of the nebula surface brightness between the two ends (facing and opposite the star) of the  $L$ -aperture, and its orientation, have to be taken into account. The margin of error can be estimated by comparing the brightnesses obtained from observations at the same position with the  $L$ -aperture on the one hand, and from the  $S$ -aperture on the other hand.

The expected ratio is 7. Few nebulae were observed with the  $L$  and the  $S$  aperture. The ratio of the brightnesses in these observations ranges from 7, as expected, to 100. Although the pointing may explain part of this large factor, the exact surface brightness of a nebula, estimated by dividing the brightness of the nebula ( $F_N$  in Eq. (1)) by the solid angle intercepted by the  $L$ -aperture, may be overestimated by a factor of 10, for positions at less than a few  $10''$  to the star.

The second uncertainty in the evaluation of  $R$  comes from the radiation field.

If the starlight is extinguished between the star and the scattering volume and if material in front of the star does not compensate for this extinction, the observed value of  $R$  is superior to the exact one. Conversely, if there is more extinction between the star and the observer than between the nebula and the observer, the observed value of  $R$  will be an inflated estimate of the exact one. Table 1 shows a tendency for the observed maximums of  $R\theta^2$  to increase with the reddening of the star. This increase may in part be explained by extinction of starlight in the vicinity of the star.

## 5 Interpretation of Equation (1)

### 5.1 The variations of the brightness of a nebula with optical depth

The stars  $17\tau$  and HD 37742 have no bump and are slightly reddened ( $E(B - V) = 0.07$ , Table 1). The nebulae emissions, which have no peculiarities at  $2200 \text{ \AA}$ , can safely be attributed to scattering. The linear transformation which permits passage from the star to the nebula spectrum is to be interpreted as the slope of the surface brightness versus the optical depth curve (Fig. A.2) in the optical depth range of the spectrum.

The same should hold for nebulae with bump. Eq. (1) expresses that around the mean optical depth  $\tau_{mean}$  of the nebula and for the wavelength range under consideration,  $F_N$  variations with  $\tau_\lambda$  can be approximated using the slope of  $S(\tau)$  (Fig. A.2) at  $\tau_{mean}$ . If  $a = 1$ ,  $F_N$  grows with  $\tau_\lambda$  and  $\tau_{mean}$  must be less than  $\tau_{max}$ . If  $a = 0$ ,  $\tau_\lambda \sim \tau_{max}$ , the spectrums are close to being proportionate. Last, if  $a = -1$ ,  $\tau_{mean} > \tau_{max}$ .

The  $b$  coefficient has a remarkable property.  $a(1\mu\text{m}/\lambda) - b$  is the only source of  $F_N$  variations with  $\lambda$  and must be proportional to the proportion of scattered starlight (restricted to  $\tau_\lambda$ -values close to  $\tau_{mean}$ ), the  $y$ -axis of Fig. A.2. Hence,  $b/a$  will always correspond to the point where the slope crosses the abscissa, with ' $x$ ' scaled to be  $1/\lambda$ . If  $a = 1$ ; the slope is positive,  $\tau_{mean} < \tau_{max}$ , and  $\tau_{mean}$  increases when  $b (< 0)$  decreases (Fig. A.2). If  $a = -1$ ; the slope is negative,  $\tau_{mean} > \tau_{max}$ , and  $\tau_{mean}$  increases with  $b/a (> 0)$ , if  $\tau_{mean}$  is not too large. The  $b/a$  coefficient provides a way to classify nebulae according to their optical depths.

The spectrums of Fig. 2 are plotted by increasing optical depths, according to the considerations of the previous paragraph. Two nebulae only,  $20\tau$  nebula 2 and NGC 7023 have their spectrums in exact proportion to the spectrum of the star. These nebulae have an optical depth  $\tau_{mean}$  equal to  $\tau_{max}$ . Their surface brightness, as a function of the optical depth, is at its maximum.

There are striking relations between the optical depth and the changes in the shape of the UV spectrum of Fig. 2. Increasing the optical depth of a nebula will soften the slope of the rise between  $2200 \text{ \AA}$  and  $1300 \text{ \AA}$ . The effect can be observed by comparing the spectrums of the stars and the nebulae. Increasing the optical depth also attenuates the FUV emission. Both phenomenae are the consequences of the increase of absorption toward shorter wavelengths, and contribute to the emphasis of the bump's visual impression. It is particularly evident for CED 201.

Most of the nebulae spectrums are close to being in proportion with the illu-

minating star's spectrum: for each nebula the zero order fit to the spectrum of the star is in reasonable agreement with the spectrum of the star. It can be interpreted as  $\tau_{mean}$  values which are close to  $\tau_{max}$ .  $R$ , calculated as indicated in Section 4, must be close to  $R_{max}$ , defined in the same section.

## 5.2 The albedo and the phase function

The interpretation which is given of the Eq. (1) involves only the change in optical depth with wavelength. There is no evidence or need for a variation of the albedo or of the phase function of interstellar grains in the wavelength range [1000, 3000] Å of the IUE observations.

There is also no evidence for variations of the properties of the grains with the direction of space.

## 6 The phase function of interstellar grains in the UV

The analysis of Eq. (1), has focused on the variation of the brightness of a nebula with wavelength, which depends on variations of the optical depth only.

The effect of the phase function of interstellar grains on the brightness of a nebula will be more evident through the comparison of the brightnesses of different observations because each of these will correspond to different angles of scattering,  $\varphi$  in Fig. A.1. IUE observations are particularly useful in this respect since they provide observations of the same nebula at different angular distances to the star and observations of nebulae illuminated by different stars.

Assume an isotropic phase function.  $F_N$  will depend on the radiation field at the position of the scattering volume and not on  $\varphi$ . The large variations of the brightness with the distance to the star ( $R \propto \theta^{-2}$ , Section 4) will be justified only if  $\theta$  is proportional to the distance  $d$  of the scattering volume to the star. It implies that the nebulae are all approximately at the same distance as the star from the observer:  $d_0 \sim 0$  and  $d = D\theta$ . The surface brightness of the nebula is:

$$S = \frac{L_\star}{4\pi d^2} Sca, \quad (2)$$

with  $L_\star$  the luminosity of the star and  $Sca$  the proportion of scattered starlight by a medium of optical depth  $\tau$  in direction  $\varphi$ . For  $\tau \sim \tau_{max}$ , the simple model developed in Zagury, Boulanger and Banchet [10], shows that  $Sca_{max}$  should

be at least  $\omega e^{-1}/(4\pi)$ .  $R_{max}\theta^2$  will be found to be:

$$R_{max}\theta^2 = \frac{S_{max}}{L_*/4\pi D^2} \theta^2 > \frac{\omega e^{-1}}{4\pi},$$

$$R_{max}\theta^2 > 0.03\omega. \quad (3)$$

Even though there is some uncertainty in the observed values of  $R_{max}\theta^2$  ( $\sim 0.003$ , Section 4), isotropic scattering probably implies an albedo of at most 0.1.

This very low albedo, and the systematic configuration in which all the nebulae need to be to justify isotropic scattering, are improbable. A more likely explanation for the variation of the surface brightness with the angular distance to the star can be attributed to variations of  $\varphi$  rather than variations of  $d$ . The quick decrease of the surface brightness with  $\theta$ , i.e. with  $\varphi$ , indicates a strong forward scattering phase function. Assuming a strong forward scattering phase function, the scattering volumes are likely to be in front of the stars, in which case we have  $d \sim d_0$  (Fig. A.1).

Three independent factors will modify  $S_{max}$ : the star luminosity,  $L_*$ , the distance to the star,  $d$ , and the angle of scattering,  $\varphi$ . The surface brightness of a nebula is proportionate to  $L_*$  and to  $d^{-2}$ . The remaining dependence on  $\varphi$  will be defined by the function  $h(\varphi) = 4\pi d^2/L_* S_{max}$ . Then:

$$R_{max} = \frac{h(\varphi)L_*/d^2}{L_*/D^2} = h(\varphi) \frac{\varphi^2}{\theta^2}. \quad (4)$$

The dependence of  $R_{max}$  on  $\theta^2$  in equation 4 was e.g. verified by the observations (section 4). Concerning the observations for which  $R_{max}\theta^2$  is nearly constant ( $R_{max}\theta^2 = c \sim 3 \cdot 10^{-3}$ ), we have:  $h(\varphi) = c/\varphi^2$ . Since  $h$  does not depend on  $\theta$  this relation must be true for the range of  $\varphi$ -values considered by the observations. It suggests that the differences between the values of  $c = R\theta^2$  in Table 1 is due to errors on the estimate of either  $R$  (Section 4.1) or  $\theta$ .

Hence, the maximum surface brightness a nebula can reach in the direction  $\varphi$  from the direction of the star varies as:

$$S_{max} = \frac{c}{\varphi^2} \frac{L_*}{4\pi d^2}. \quad (5)$$

Eq. (5) applies to  $\varphi = \theta D/d$  values between a few  $10''$  (or less) and a few  $10'$ .

## 7 Further implications

### 7.1 The UV spectrum of the stars

An important consequence of the relation found between the spectrum of the nebulae and the spectrum of the illuminating stars concerns the 2200 Å bump.

In none of the UV observations of the nebulae presented here is there evidence for the presence of the 2200 Å carriers. If starlight is not affected by the presence of the bump carriers when the nebula is on the side of its illuminating star, why should it be affected when the nebula is in front of the star?

From Eq. (5) it is clear that considerable starlight can be scattered into the beam of the telescope at close angular distance to a star. If  $\varphi_{min}$  is the smallest angle down to which Eq. (5) holds, and if we assume  $R_{max}$  to be constant for  $\varphi < \varphi_{min} = \theta_{min}D/d$ , the proportion of starlight scattered into the beam of semi angle  $\theta_0$  can reach:

$$\int_0^{\theta_0} 2\pi R_{max} \theta d\theta = \int_0^{\theta_{min}} \frac{2\pi c \theta}{\theta_{min}^2} d\theta + \int_{\theta_{min}}^{\theta_0} \frac{2\pi c}{\theta} d\theta$$
$$= \pi c \left( 1 + 2 \ln \left( \frac{\theta_0}{\varphi_{min}} \frac{D}{d} \right) \right) \quad (6)$$

$$\sim 10^{-2} \left( 1 + 2 \ln \left( \frac{\theta_0}{\varphi_{min}} \frac{D}{d} \right) \right) \quad (7)$$

It can easily be a few percent of the direct starlight corrected for extinction. The proportion of scattered starlight into the beam will be even more important when compared to the direct starlight  $F_\star$  received by the telescope, since the latter is extinguished.

The implication may be that there are no bump carriers. It was noted by Bless & Savage [1] (see also Cardelli & Clayton [5] pp. 519 and 520) that the bump will also be explained if enough starlight scattered in the beam of the observation was added to the direct starlight. This possibility was ruled out (Bless & Savage [1]) on the basis of arguments which do not hold if grains strongly scatter light in the forward direction.

## 7.2 *Interstellar grains properties*

### 7.2.1 *Albedo and phase function*

Contrary to Witt [7], who finds variations of grain properties in one direction to another, I find homogenous properties of interstellar grains in all directions and constant albedo and phase function in the UV.

Witt & Bohlin [8] claim the discovery of enhanced scattering emission in reflection nebulae associated with the 2175 Å extinction band but no such irregularities can be observed in any of the nebulae presented here. The spectrums of CED 201 and IC 435 presented in Witt & Bohlin are close to the raw data which may mean they have not been treated according to IUE most recent recommendations. Consequently, large differences exist between the nebulae spectrum in Witt & Bohlin and the ones presented at the IUE website and reproduced here. The long wavelength range observation of CED 201 used by the authors, LWR 17725, on which most of their discussion relies, is classified ‘*a/n*’ or ‘abnormal reading’ and ‘non standard acquisition’ at INES Archive Data Mirror.

The spectrums of IC 435 and CED 201 presented in Fig. 2 are an average of the best observations of the nebulae, most of which were not available at the time Witt & Bohlin did their work. The spectrums have no unique features, except for the large optical depth met in CED 201. It is most probable that Witt & Bohlin’s analysis as well as their conclusions are questionable.

Another study, the Calzetti et al. [4] paper on IC 435, uses the same data as that found in the present paper. The authors have followed the Witt & Bohlin analysis and attribute the variation of  $\log(S_N/F_\star)$  with wavelengths to changes in the albedo and/or phase function of the grains. They didn’t search for a relation between the star flux, the nebula surface brightness and  $1/\lambda$ .

### 7.2.2 *Power law dependance of the surface brightness on $\theta$*

The power law dependence of the surface brightness of NGC 7023 with distance to the star was investigated from the optical to the UV by Witt & Cottrell [6] and Witt et al. [9].

The power law which is found in these two papers has an exponent  $\sim 1.5$  in absolute value, smaller than the one found in this paper. This exponent is not the one which can be deduced from the raw data since the authors try to include a correction for the width of the aperture, which introduces an error on the surface brightness estimate at close angular distance to the star.

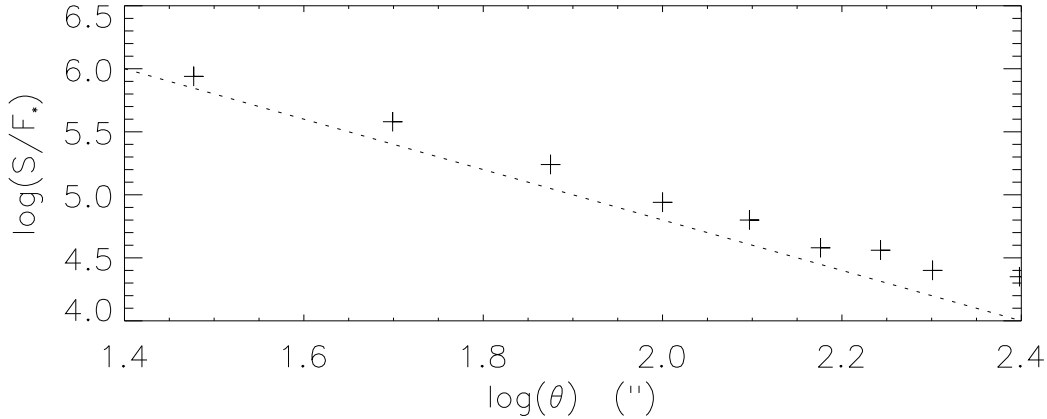


Fig. 3.  $\log(S/F_*)$  versus  $\log \theta$  from the observations of Witt & Cottrell [6], table II, field North. The dotted line has a slope of  $-2$ . The same dependence of  $S/F_*$  on  $\theta^{-2}$  is found for the other fields (W, S, E).

The raw data are not given in Witt et al. [9]. The observational results given in Witt & Cottrell [6] for the optical wavelengths give an exponent of 2 (Fig. 3). Other observational data, for instance the Witt & Schild [8] study of fifteen reflection nebulae, give a similar exponent (Zagury, submitted).

Precise comparison of the different papers cannot be broached here. An exponent of 2 is logical within the present analysis. The exponent of 1.5 found in Witt et al. [9] is also justified by the model developed in their paper.

Another idea which emerges from the comparison of the data in the different papers mentioned in this section, is that the UV and optical wavelengths for which  $R\theta^2$  can be calculated give similar values. If true, it may imply similar properties (albedo and phase function) of interstellar grains from the near infrared to the far UV.

## 8 Conclusion

Comparison of the UV spectrum of several nebulae observed by the IUE satellite to the spectrum of the illuminating stars shows that the spectrum of a nebula is always the product of two terms: the flux of the star  $F_*$  and a linear function of  $1/\lambda$ . This function was interpreted as the slope of the surface brightness  $S$  of the nebula versus optical depth at the optical depth  $\tau_{mean}$  of the nebula. The variation of  $R = S/F_*$  with wavelength, and of its maximum with the angular distance  $\theta$  to the star, provides additional informations on the properties of interstellar dust and on the nebulae.

The linear  $1/\lambda$  function gives an estimate of  $\tau_{mean}$ , since the slope of  $S(\tau)$  decreases with  $\tau$ . It allows a classification of the nebulae according to their

mean optical depth. For all the nebulae of the sample,  $\tau_{mean}$  should be close to  $\tau_{max}$ , the optical depth at which maximum surface brightness is reached. This is in conformity with the high brightnesses of the nebulae.

The important variations of the ratio  $R = S/F_{\star}$  with the angular distance  $\theta$  to the star is explained if the interstellar grains have a strong forward scattering phase function in the UV.

In some observations the maximum value of  $R$ ,  $R_{max}$  varies as  $1/\theta^2$ . This result is justified if the phase function is so that  $R_{max}$  is proportional to  $1/\varphi^2$ , where  $\varphi$  is the angle of scattering.

No additional absorption or other particular behaviour at 2200 Å was noticed in the spectrum of the nebulae. The absence of bump carriers in the nebulae calls to question the interpretation of the 2200 Å bump in the spectrum of the stars. When a star is observed behind a nebula a considerable amount of starlight scattered into the beam can be added to the direct starlight and may explain the bump.

The understanding and interpretation we have reached of the UV spectrum of nebulae applies similarly to different regions of the interstellar medium. It indicates that the UV properties (albedo and phase function) of interstellar grains are identical in all directions of space. These properties may be the same from the near infrared to the far UV.

## A Appendix: Variations of a nebula surface brightness with optical depth

Elementary properties of scattering used in this paper are summarized by the plot of Fig. A.2. The plot represents surface brightness variations with optical depth for a cloud illuminated by a far away source (the source of light comes from one direction).

The  $x$ -axis of the plot is the optical depth, related to the quantity of interstellar grains photons have crossed on their way to the telescope. The optical depth depends on wavelength and on the column density along the path the photons have followed. Optical depth and column density are proportional. Optical depth is a linear function of  $1/\lambda$ . Thus, depending on the kind of observation which is involved, spectroscopy or photometry,  $\tau$  will vary from a point to another according to the wavelength or to the quantity of matter on the photons' way. The quantity of matter on the photons' way depends on the angle made by the observer, the source radiation field and the nebula. Only for directions close to the illuminating source can  $\tau$  be assimilated to



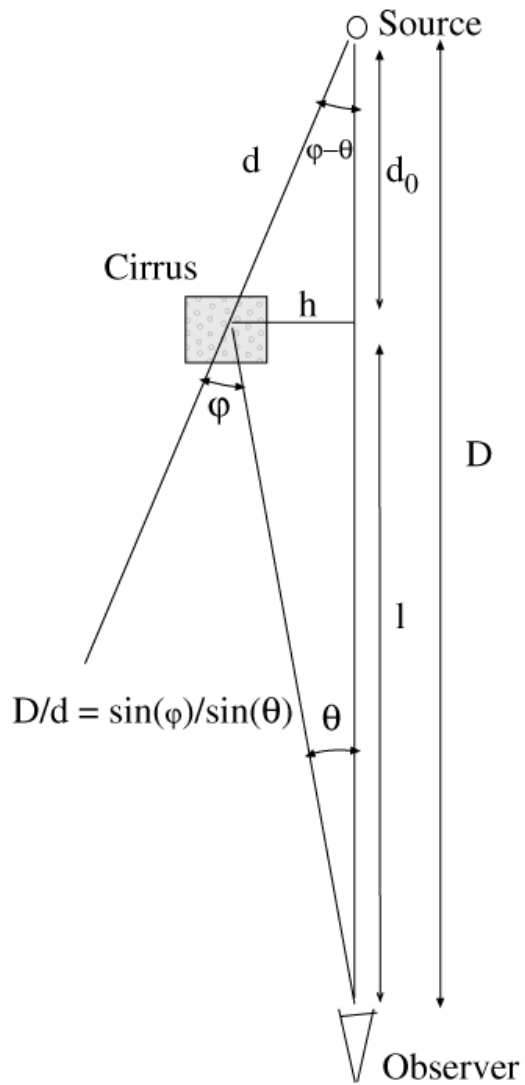


Fig. A.1. Representation of the angles employed in the text.

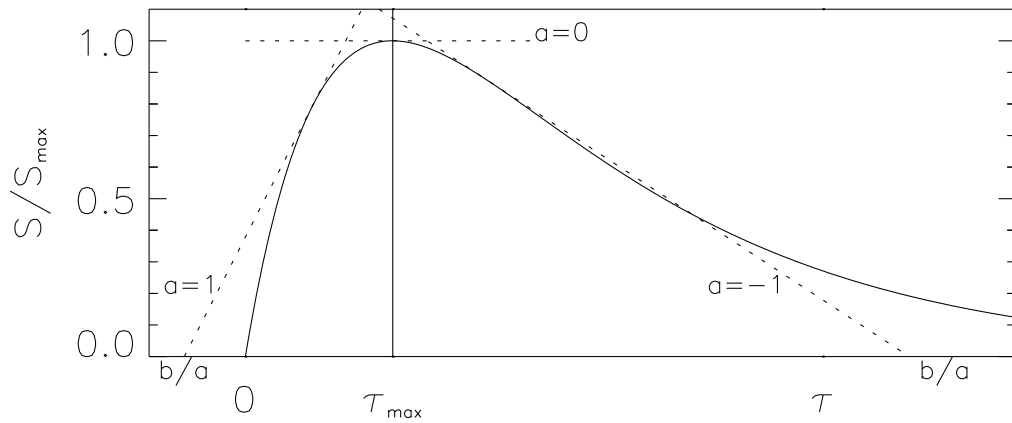


Fig. A.2. Surface brightness (scaled to 1 at maximum) versus optical depth.

the cloud column density.

The  $y$ -axis is the nebula surface brightness scaled to 1 at maximum surface brightness. At very small  $\tau$ , variations of  $S$  and  $\tau$  are proportional. Absorption will quickly diminish the slope  $dS/d\tau$ .  $S$  will have a maximum at a value  $\tau = \tau_{max}$  and decreases for  $\tau > \tau_{max}$ . For any given column density, there is a wavelength at which  $\tau = \tau_{max}$  is reached and reciprocally. Hence there is a correspondence between wavelengths and column densities which allow to predict at which wavelength a cloud will preferably be observed and the possible range of column densities of a cloud bright in a certain wavelengths range.

For a constant albedo,  $S_{max} = S(\tau_{max})$  should depend solely on the phase function, i.e. only on the angle  $\varphi$  of the source radiation field direction with the direction of the scattering volume and the observer.

## Acknowledgements

I thank Professor Y. Fukui for the support and freedom I took benefit from during two years in Japan and without which this work would not have been possible. I received constant help and a warm welcome from all the Radio Astronomy group of Nagoya University. A special thank to Dr Onishi and to Dr Mizuno.

Dr E. Soleno, from ESA, introduced me to the use of the IUE data and answered many questions. I am also indebted to Stacey Young for having reviewed many times the english of the manuscript.

## References

- [1] Bless R.C., Savage B.D, 1972, ApJ, 171, 293
- [2] Boggess A., et al., 1978, Nature, 275, 372
- [3] Boggess A., et al., 1978, Nature, 275, 377
- [4] Calzetti D., et al., 1995, ApJ, 446, L97
- [5] Cardelli J.A., Clayton G.C., 1988, AJ, 95, 516
- [6] Witt A.N., Cottrell 1980, A.J., 85, 22
- [7] Witt A.N., 1985, ApJ, 294, 216
- [8] Witt A.N., Bohlin R.C, 1986, ApJ, 305, L23

[9] Witt A.N., et al., 1992, ApJ, 395, L5

[10] Zagury F., Boulanger F., Banchet V., 1999, A&A, 352, 645